OPEN

Experimental & Molecular Medicine (2016) 48, e274; doi:10.1038/emm.2016.105

www.nature.com/emm

ORIGINAL ARTICLE

Optimization of the optical transparency of rodent tissues by modified PACT-based passive clearing

Jiwon Woo[1], Mirae Lee[2], Jeong Min Seo[3], Hyo Suk Park[1] and Yong Eun Cho[1]

Recently, a bio-electrochemical technique known as CLARITY was reported for three-dimensional phenotype mapping within transparent tissues, allowing clearer whole-body and organ visualization with CB-perfusion (CUBIC) and leading to the development of whole-body clearing and transparency of intact tissues with the PACT (passive clarity technique) and PARS (perfusion-assisted agent release *in situ*) methodologies. We evaluated the structure–function relationships in circuits of the whole central nervous system (CNS) and various internal organs using improved methods with optimized passive clarity. Thus, in the present study, we aimed to improve the original PACT procedure and passive clearing protocols for different intact rodent tissues. We determined the optimal conditions for the passive clarity method that allowed the production of a transparent whole CNS by clearing the brain and spinal cord, as well as various organs. We also improved the tissue transparency using mPACT (modified PACT), a method for direct passive clearing, and whole perfusion-based PARS-mPACT, a method for fusion clearing, and we identified the appropriate experimental conditions. These optimized methods can be used for easy and economical high-resolution mapping and phenotyping of normal and pathological elements within intact tissues.
Experimental & Molecular Medicine (2016) **48,** e274; doi:10.1038/emm.2016.105; published online 2 December 2016

INTRODUCTION

Clear Lipid-exchanged Acrylamide-hybridized Rigid Imaging-compatible Tissue-hYdrogel (CLARITY) tissue-clearing technologies create optically transparent images that provide advances in biological systems.[1,2] The CLARITY and passive clarity technique (PACT) methods improve tissue permeability by replacing the lipid bilayer of the plasma membrane with a hydrogel.[3,4] These methods preserve the intact structure of the brain, allowing the projection of nerve tracts along with three-dimensional (3D) and topological reconstruction.

CLARITY promotes an accelerated rate of clearing in undissected tissues via electrodynamic force.[1] PACT and PARS (perfusion-assisted agent release *in situ*) can also generate optical transparency in the brain and internal organs through a perfusion-based passive clearing technique.[3,4] Additional methodologies for clearing tissue have also been reported, such as Sca*l*e[3] SeeDB,[4] Clear*T*,[5] CUBIC[6] and SWITCH.[7]

The CLARITY technique employs strong electronic forces that may potentially cause tissue damage; however, a recent report has suggested that a supply of optimized electrophoretic tissue clearing (ETC) conditions with 250 and 280 mA reduces such risk.[8] Furthermore, PACT can easily produce optical transparency and reduce tissue damage in the mouse brain and other organs, but these features require more time.[9,10] Currently, the technique has not been widely implemented to achieve the clearing of larger model organisms, such as rats and guinea pigs.

Furthermore, a number of studies have reported limitations in achieving optical transparency in specific regions in the central nervous system (CNS); tissue-clearing techniques have also not yet been applied to the whole CNS form. The present study proposes novel methodology for facilitating the fast clearing of the whole CNS and internal organs using systemic and cerebrospinal circulation.

We sought to reduce the time needed for the passive clearing conditions of the existing PACT. We particularly focused on the blood vessel patterns of all organs using confocal microscopy. This study suggests that tissue clearing is useful and easily applied to the physiological and anatomical evaluation of the vascular system in various tissues of a diverse assortment of animals.

[1]The Spine and Spinal Cord Institute, Department of Neurosurgery, Gangnam Severance Hospital, Yonsei University, Seoul, Republic of Korea; [2]Division of Nephrology, Department of Internal Medicine, Gangnam Severance Hospital, Yonsei University, Seoul, Republic of Korea and [3]Cellular Reprogramming and Embryo Biotechnology Laboratory and Dental Research Institute, Seoul National University School of Dentistry, Seoul, Republic of Korea
Correspondence: Dr YE Cho, The Spine and Spinal Cord Institute, Department of Neurosurgery, Gangnam Severance Hospital, Yonsei University, Seoul 06273, Republic of Korea.
E-mail: yecho@yuhs.ac
Received 18 April 2016; revised 22 June 2016; accepted 27 June 2016

MATERIALS AND METHODS

Experimental animals

Adult male C57BL/6 mice (25–30 g) were purchased from Koatech Inc. (Gyeonggi-Do, Korea), and adult male SD rats and male Hartley guinea-pigs (250–350 g) were purchased from Orient Inc. (Gyeonggi-Do, Korea). Mouse embryos were isolated on day 13.5 of pregnancy in BALB mice obtained from the Laboratory Animal Research Center of Yonsei University (Seoul, Korea). All experimental procedures involving animals were conducted in accordance with the animal resource guidelines of Yonsei University.

Passive clarity

Perfusion of experimental rodents. After anesthesia, the thorax of various types of rodents (mouse, rat and guinea pig) was opened, and an incision was made in the right atrium of the heart. Perfusion washing was performed with equal volumes of cold 0.1 M phosphate-buffered saline (PBS) containing 10 unit ml^{-1} heparin (volume for mice: 20 ml, for rats and guinea pigs: 200 ml) and cold 4% paraformaldehyde (PFA) solution using a 50-ml syringe. The CNS was rescued following the standard methods.

Modification of PACT. Cultures were established from the whole CNS (brain and spinal cord) and organs from the fixed bodies of mice and rats on a clean bench. Each tissue was transferred to sufficient 4% PFA solution to cover the tissue in a 50-ml tube and stored at 4 °C for 24 h. Fixed tissue was washed for 1 h with 0.1 M PBS in a 50-ml tube and then transferred to sufficient enough A4P0 solution (4% acrylamide in PBS) to cover the tissue in a 50-ml tube at 37 °C for 24 h. Next the tissue was covered with 0.25% VA-044 (Wako Pure Chemical Industries Ltd., Osaka, Japan) in 0.1 M PBS in a 50-ml tube at room temperature for 6 to 24 h. After treatment with VA-044, the samples were embedded with nitrogen gas for 10 min, and the tissue was transferred to a 50-ml Falcon tube containing sufficient clearing solution (8% sodium dodecyl sulfate (SDS) in 0.1 M PBS, pH 8.0) with 0.5% α-thioglycerol (Sigma-Aldrich, Inc., St Louis, MO, USA) to cover the tissue; the sample was then incubated with shaking at 150 r.p.m. for 37 °C until the tissue cleared.

Combined PARS-mPACT. Each perfused fixed body was transferred to a perfusion chamber for whole-body perfusion through the right atrium of the heart via an 18-gauge needle that was connected to a peristaltic pump. Fluid was circulated through the body at a velocity of 10 ml min^{-1}. The wash began with 100 ml of 4% PFA for 4 h at room temperature in the chamber, followed by washing with 100 ml of 0.1 M PBS for 3 h under the same conditions. Next 200 ml of A4P0 solution was circulated throughout the body for 2 h. The infused body was then incubated for 3 h at 37 °C to degas for 2 min under nitrogen gas and polymerized by the perfusion of 200 ml of recirculating 0.25% VA-044 in PBS for 3 h. The whole CNS (brain and spinal cord) and various organs were extracted from each body on a clean bench. The whole CNS was extracted as previously reported. The extracted tissues were transferred to clearing solution (8% SDS, 0.5% α-thioglycerol in 0.1 M PBS) in a 50-ml tube and incubated with shaking at 150 r.p.m. for 37 °C until visible clearing of the tissue was observed. Rat leg bones lacking lipid clearing after the PARS method were subject to decalcification (deCAL) five times over 15 days with 50 ml of Calci-Clear Rapid decalcifying solution (National Diagnostics, Atlanta, GA, USA), which was changed after 4 days. The decalcified bones were prepared according to the modified PACT (mPACT) method and were cleared and mounted with Nycodenz-based refractive index media solution (*n*RIMS) solution. For further instructions, refer to Supplementary Figure 3.

Clarity

The adult rat body was perfused with 200 ml of cold 0.1 M PBS solution, followed by 200 ml of cold hydrogel solution with a mixture (cold 4% PFA, 4% acrylamide, 0.05% bis-acrylamide and 0.25% VA-044 in 0.1 M PBS) using a 50-ml syringe. The CNS was retrieved following standard methods and incubated in fresh hydrogel monomer solution at 4 °C for 1 day. The hydrogel solution was embedded with nitrogen gas for 10 min and polymerized by incubation for 3 h at 37 °C. The CNS was removed from excess hydrogel and placed in an ETC chamber. The clearing solution (4% SDS and 200 mM boric acid, pH 8.5) was circulated at a velocity of 2 l min^{-1} though the ETC chamber and the connected circulator (ECO RE-415, LAUDA-Brinkmann, Lauda-Königshofen, Germany), and 30 V was applied for 1–2 weeks at 37 °C.

*n*RIMS imaging media with RI 1.46

The cleared tissue was gently washed in 0.1 M PBS for 1 h and transferred to a new tube containing *n*RIMS solution and 0.8 g ml^{-1} Nycodenz (Axis-Shield Density Gradient Media, Oslo, Norway) in 30 ml of base buffer (0.01% sodium azide and 0.1% Tween-20 in 0.1 M PBS, pH 7.5). All tissues were incubated in *n*RIMS solution for 2–10 days or until they became transparent at room temperature. All clear images of tissues were captured using a digital camera (SM-G925S, Samsung Electronics Co., Ltd, Suwon, Korea).

Immunostaining and preparation for imaging

*n*RIMS-treated tissue was washed with 0.1 M PBS for a period of 5 h to overnight until *n*RIMS clearing occurred. Each washed tissue was sectioned into 4-mm-thick sections with a blade. All clarified tissue was then incubated with 0.1% Triton X-100 (Sigma-Aldrich) in 0.1 M PBS for 2 h and blocked with 2% bovine serum albumin in 0.1 M PBS for 6 h. Immunostaining was performed for 2 days using a primary anti-rabbit CD31 antibody (1:100, Santa Cruz Biotechnology Inc., Dallas, TX, USA) after three washes with PBST (0.1% Tween-20 in 0.1 M PBS) solution for 2 h. Next sections were incubated with a secondary antibody goat anti-rabbit-IgG Cy3 fluorescent conjugate (1:500, Jackson ImmunoResearch Inc., West Grove, PA, USA) in 2% bovine serum albumin for 2 days. The labeled tissue was washed three times with PBST solution for 2 h and stored in 15 ml of *n*RIMS solution for 2–10 days. Before imaging, the Cy3-labeled tissue was moved and fixed with a small amount of *n*RIMS solution on 35- or 60-mm tissue culture dishes with silicone around the bottom edge of the dish. Next 1.5–2 ml of fresh *n*RIMS solution was added, and the dish was covered. For further instructions, refer to Supplementary Figure 2.

Image processing of 3D images

Images of cleared tissues were acquired with tile scanning using an LSM-780 confocal laser scanning microscope (Cal Zeiss, Jena, Germany) with ×10 magnification and the Zeiss software. The videos were edited to serial images using the Vegas Pro 12.0 software (Sony Corporation, Tokyo, Japan).

RESULTS

Generation of a transparent model of the CNS and internal organs using a modified passive clearing technique

For postpolymerization clearing of the hydrogel-embedded rat CNS samples, an electric field was applied in an ETC. Although

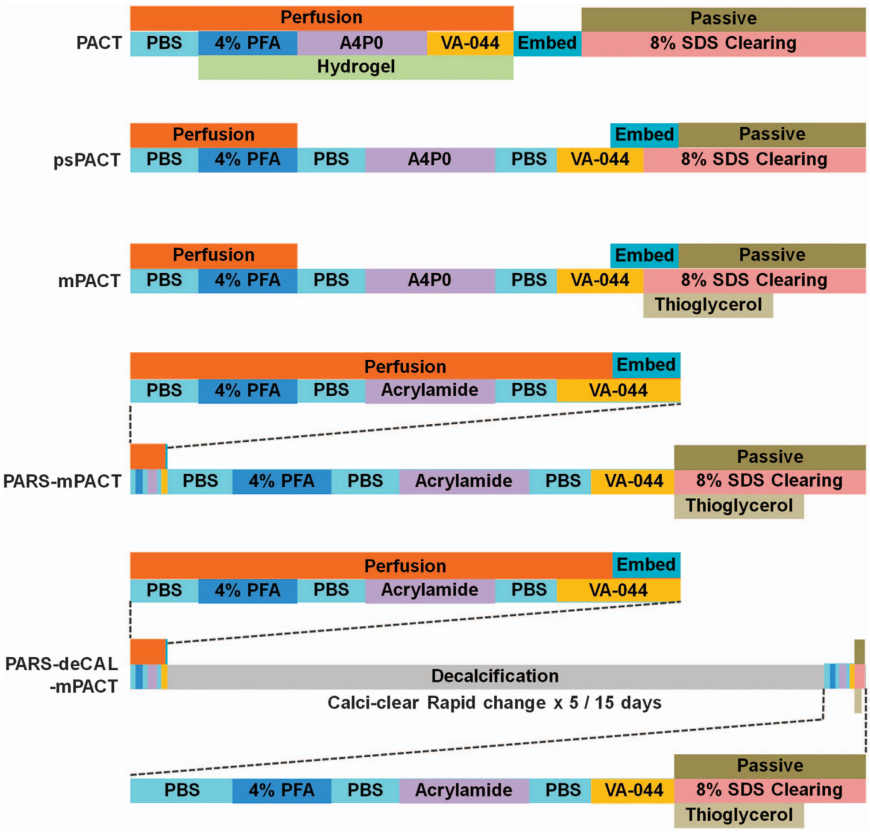

Figure 1 Schematic representation of modification of passive clearing methods. The individual reagents used for polymerization in the PACT-based methods are shown, as well as the polymerization step used to conduct the passive clearing step in this study. The boxes in parentheses indicate the steps of the designed method.

previous studies recommended using a high voltage (30 V), this level was found to cause discoloration and the deposition of black particles in treated rat CNS samples (Supplementary Figure 1). To address this issue, we optimized the parameters involved in using PACT to clear CNS samples.

As shown in Figure 1, transparent tissue was rapidly created with passive clearing under different conditions. psPACT (process-separate PACT) used separate treatment processes of 4% acrylamide (A4P0) solution and 0.25% VA-044 initiator solution for the hydrogel formation of the tissue; these conditions differed from those of the original PACT method. mPACT added 0.5% α-thioglycerol, as in the previously reported SeeDB method,[4] to the 8% SDS clearing solution of the psPACT method. For both methods, the intact tissues were incubated in 37 °C shaking incubator until maximal clearance was achieved. As shown in Figure 2a, psPACT cleared the entire CNS in 20 days, while PACT required 23 days. In contrast, mPACT rapidly and thoroughly cleared the whole CNS in just 14 days. Each cleared mouse CNS was incubated in *n*RIMS mounting media until transparent. Day 14 samples processed via psPACT and mPACT are compared and presented in Figure 2b.

To investigate the major blood vessels in the whole organism, the microvasculature of the mouse spinal cord was stained using anti-CD31 mouse and Cy3-conjugated antibodies and was subsequently examined using confocal microscopy (Figure 2c). In addition, blood vessel images were analyzed using the rat brains that were cleared via mPACT (5 days), psPACT (7 days) and the original PACT (10 days) and subsequently processed into 4-mm thick sections (Figures 2d–g).

Next the optimal passive clearing conditions for the whole internal organs of adult mice were determined for mPACT, psPACT and the original PACT. Whole liver samples were cleared with mPACT (18 days), psPACT (20 days) and the original PACT (22 days) (Figure 3a). Whole lung samples were cleared with mPACT (14 days), psPACT (14 days) and the original PACT (18 days) (Figure 3b). The heart, stoma, salivary gland and pancreas achieved clarity after 15–17 days with mPACT, and they cleared after 17–21 days with psPACT and the original PACT (Figures 3c–f).

Using these passive methods, we were able to visualize intact, transparent models of the whole CNS and various organs, although the clearing times differed among the three methods (Supplementary Table 1). The optimized passive clearing methods achieved organ clarity in a shorter length of time (Supplementary Table 1). Taken together, these results suggest that the mPACT clearing method can generate clear organs more stably and rapidly than the previous passive clearing methods.

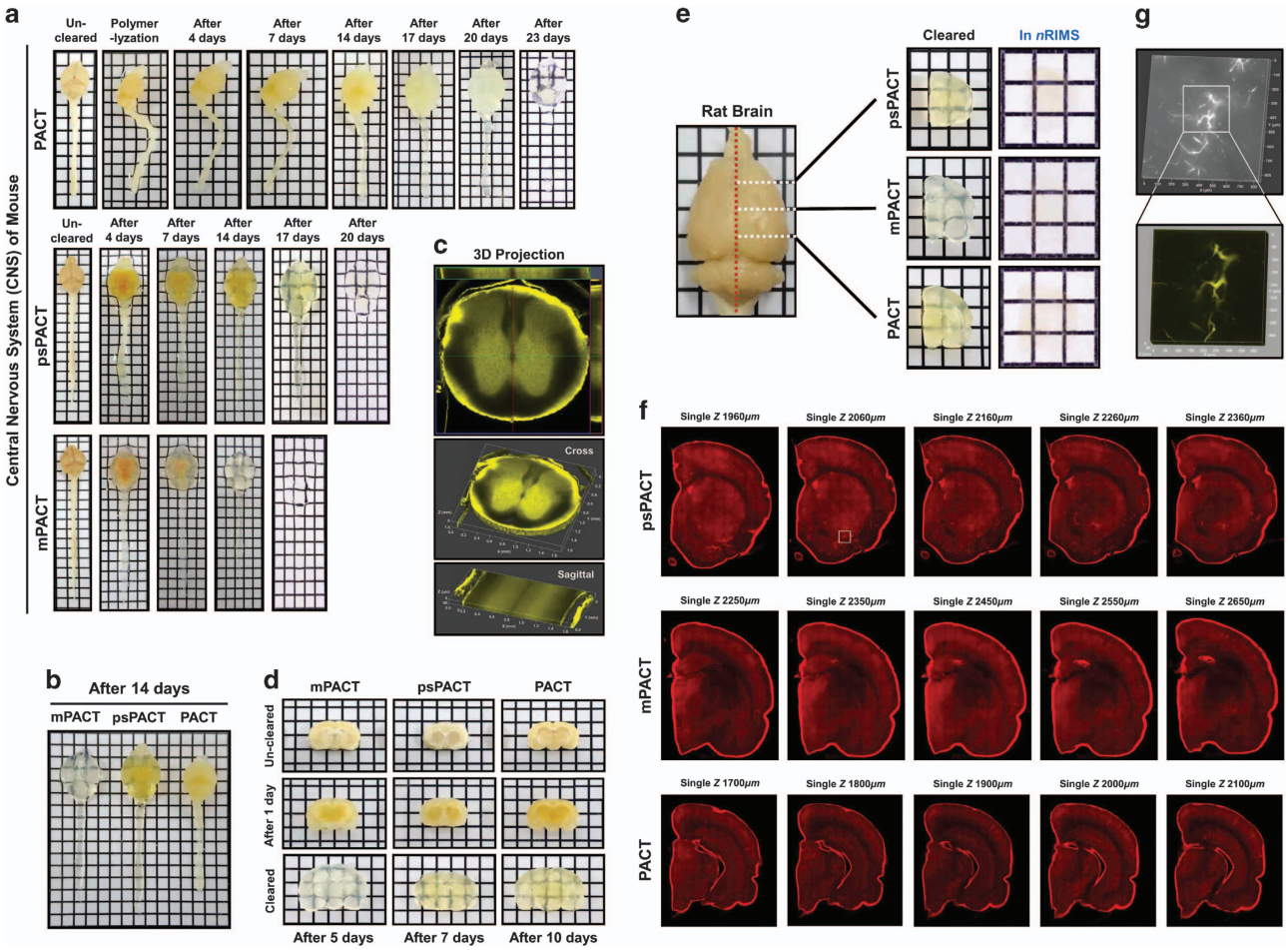

Figure 2 Mouse CNS clearing performance and comparison of modified methods. (**a**) The optical transparency was compared for the whole CNS of adult mice using psPACT, mPACT and PACT. Left, CNS washed with PBS after fixation with 4% PFA. All CNS images were produced with a black cross lattice (width 5 mm) as the background on the clearing day. (**b**) Comparison of the three methods in whole CNS of mice cleared after 14 days by mPACT (left), psPACT (middle) and original PACT (right). (**c**) Visualization of CD31 labeling the intact mouse spinal cord with mPACT. We acquired 4 (2 × 2, horizontal × vertical tiles) tiled scans of each cross-section and 2 tiled scans of the sagittal section, and then we constructed 3D projection images (100 μm steps) using *z*-stacking. (**d**, **e**) Comparison between the three methods in 4-mm-thick rat brain samples: mPACT, psPACT and the original PACT. The clearing results of rat brain section are shown in (**d**). The transparency of all cleared samples was evident against a patterned background (length:width = 5 mm:5 mm). The samples were stained with anti-CD31 and Cy3 antibodies and incubated in *n*RIMS. The transparency of all cleared samples was evident against a patterned background (length:width = 5 mm:5 mm). (**f**) The whole image of each sample was created from serial single *z*-images (*z* = 1700–2650 μm) of the blood vessel pattern using a confocal microscopy and (**g**) from the 3D projection image (z = 90 μm) of a focused blood vessel in the brain of psPACT.

Generation of transparent mouse embryos

To assess the sufficiency of tissue clearing, mouse embryos were processed via mPACT at various stages of embryonic development. The embryos at stages E9.5, E10.5, E11.5 and E13.5 were easily cleared by mPACT in 3 days (Figure 4a), and the transparency was evident against a patterned background.

To investigate the initiation of the angiogenesis process of the notochord in embryos, the blood vessel patterns that are important for spine generation in mouse development were examined using anti-CD31 antibodies and confocal microscopy. We successfully generated *z*-stack images of the blood vessel pattern in the notochord of the tail region at embryonic day 11.5 (Figure 4b). The data from the clear embryo models indicate that the mPACT method can be used to clear embryos of diverse developmental stages without ETC. The transparent embryos facilitated the use of 3D-phenotypic analysis to study angiogenesis during embryogenesis.

Generation of a transparent CNS and organs through perfusion-based passive clearing techniques

The present study also sought to apply the aforementioned passive tissue clearing methods in larger model organisms. The whole perfusion technique is noteworthy in that it increases the transparency of the whole body and internal organs, as with the CB-perfusion method.[11] Therefore we analyzed whether the combination of our mPACT method and PARS could also improve whole-body perfusion methods (Figure 1). The PARS-mPACT method was based on the experimental

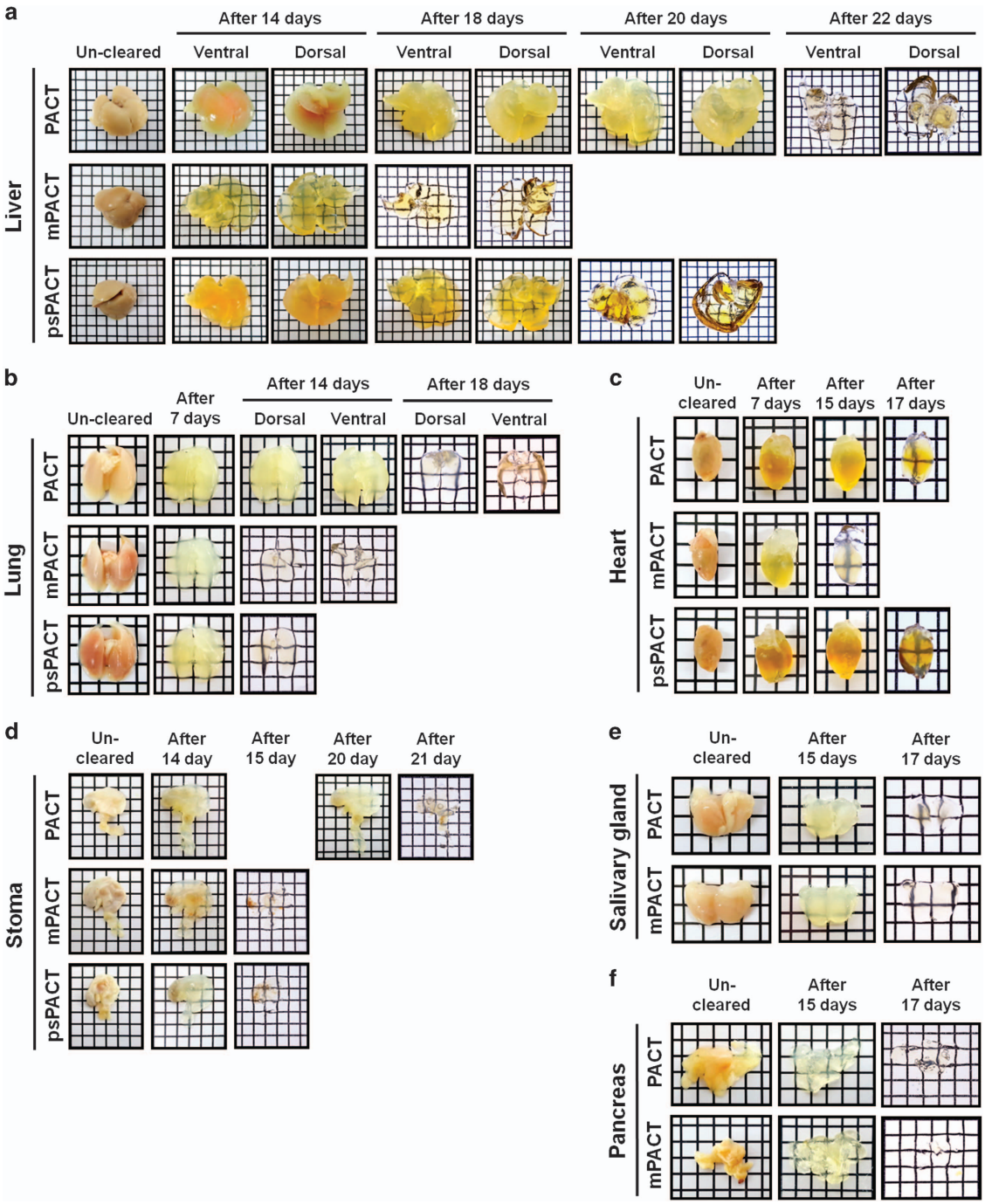

Figure 3 Clearing performance for mouse internal organs and comparison of the modified methods. The optical transparency was compared in the adult mouse (**a**) whole liver, (**b**) whole lung (ventral and dorsal), (**c**) heart, (**d**) stoma, (**e**) salivary gland and (**f**) pancreas following PACT, mPACT and psPACT clearing. Left, the organ washed with PBS after fixation with 4% PFA. The transparency of all cleared samples was evident against a patterned background (length:width = 5 mm:5 mm).

conditions of the whole perfusion and mPACT passive clearing methods (Supplementary Figure 3).

Tissues were initially subjected to PARS and were fixed via transcardial perfusion of 1% PBS with 100 unit ml^{-1} heparin and 4% PFA, as well as whole perfusion of 4% acrylamide solution and 0.25% VA-044 in PBS, for 2 days by peristaltic pump. Polymerized tissues were then isolated and passively cleared according to the mPACT protocol.

A comparison of the optical transmittance achieved with PARS-mPACT and mPACT alone showed that overall transparency of the whole rat CNS was achieved after 21 days (Figure 5a). We confirmed that the brain tissue cleared by PARS-mPACT maintained resilience. No remarkable differences were identified between the two methods based on the appearance of the whole rat CNS. Imaging of blood vessel patterns was performed, focusing on the lumbar spinal

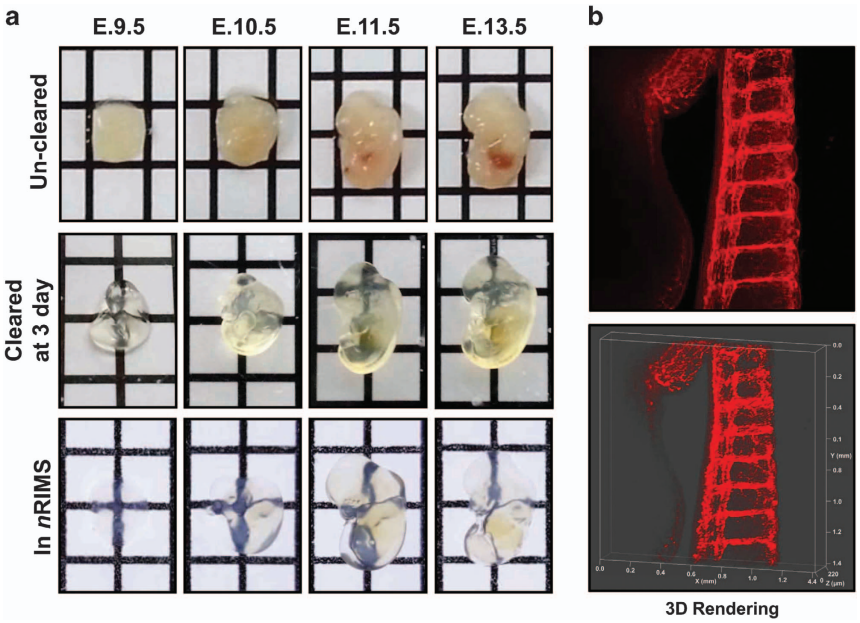

Figure 4 mPACT-cleared mouse embryos during developmental stages. (**a**) Photo of cleared mouse embryos (E9.5 E10.5, E11.5 and E13.5) captured with a black cross lattice (width 5 mm) as the background. All embryos were mPACT-cleared for 3–4 days. (**b**) Tail region visualization of a CD31-labeled embryo (E11.5) cleared with mPACT. We acquired 3D projection images (220 μm steps) using a ×10 objective lens and *z*-stacked them. The yellow arrow indicates a blood vessel of the tail. The transparency of the cleared embryos was evident against a patterned background (length:width = 5 mm:5 mm).

nerve region, including the cauda equina (Figure 6a, and Supplementary Movies 5 and 6). The guinea pig CNS required 25 days for clearing by PARS-mPACT (Figure 5b), which was expected owing to its larger size.

Additional organs were extracted and further cleared by PARS-mPACT and mPACT. PARS-PACT, PARS-mPACT and mPACT processing of the kidney all resulted in clearing after 23 days (Figure 5c). The spleen, parotid gland, pancreas and whole lung cleared after approximately 15–19 days (Figures 5d–g). In both rats and guinea pigs, the heart cleared after 16 days (Figure 5h). The salivary gland and whole genital organs cleared after approximately 18–20 days (Figures 5i and j). Finally, the whole liver cleared after 23 days (Figure 5k and Supplementary Table 1). In addition, we processed whole blood vessel images in the whole organism, as well as the microvasculature of the rat spleen, the caudal lobe and the kidney (Figures 6b–d, and Supplementary Movies 1 and 2).

These results suggest that the PARS-mPACT clearing method improves dimensional stability by dual processing, enabling clearing deep within large and pigmented organs.

Clearing of rat bone using a PARS-mPACT-based method

To allow for the clearance of rat bone and subsequent imaging of major blood vessels in decalcified bone samples, we developed a whole perfusion-based PARS-deCAL-mPACT fusion method. This technique facilitated passive clearing of the tibia bones by PARS, mPACT and deCAL. For this method, the leg bone was removed from the muscle and decalcified for 15 days as an intermediate step and then mPACT method was used (Figure 1). Our study successfully generated a clear rat leg bone (Figure 7a) and obtained *z*-stack images of the blood vessel pattern of the sagittal aspects of the tibia and fibula (Figures 7b–d and Supplementary Movies 3 and 4), as well a cross-section of the tibia (Supplementary Figure 4). These experiments demonstrate that the PARS-mPACT method can be used to generate transparent models of any bone by whole perfusion, expanding the opportunities for 3D anatomical analysis.

DISCUSSION

The PACT has proven useful for investigating the pathology of intact organs; however, this technique has several shortcomings.[9,10] Although PACTs require limited equipment and minimal hands-on processing time, they require long time to achieve maximal tissue clarity. In the present study, we were able to generate mPACT protocols that significantly reduced the time required for tissue clearing (Supplementary Table 2). This study successfully established a modified psPACT method that allows hydrogel tissue processing of tissue in a mixed solution of reagents. The advantages of such an approach include relatively fast clearing, soft tissue gelation and less damage to tissues. In addition, this study also developed a second modified method that enables deep visualization within cleared tissues without any damage; this method, named mPACT, involves the addition of α-thioglycerol to the 8% SDS clearing solution. In addition, although previous studies have achieved clearing of the brain, none have reported clearing of the whole mouse CNS. Applying PACT method to the whole mouse CNS allows visualization of the whole neural network using 3D imaging.

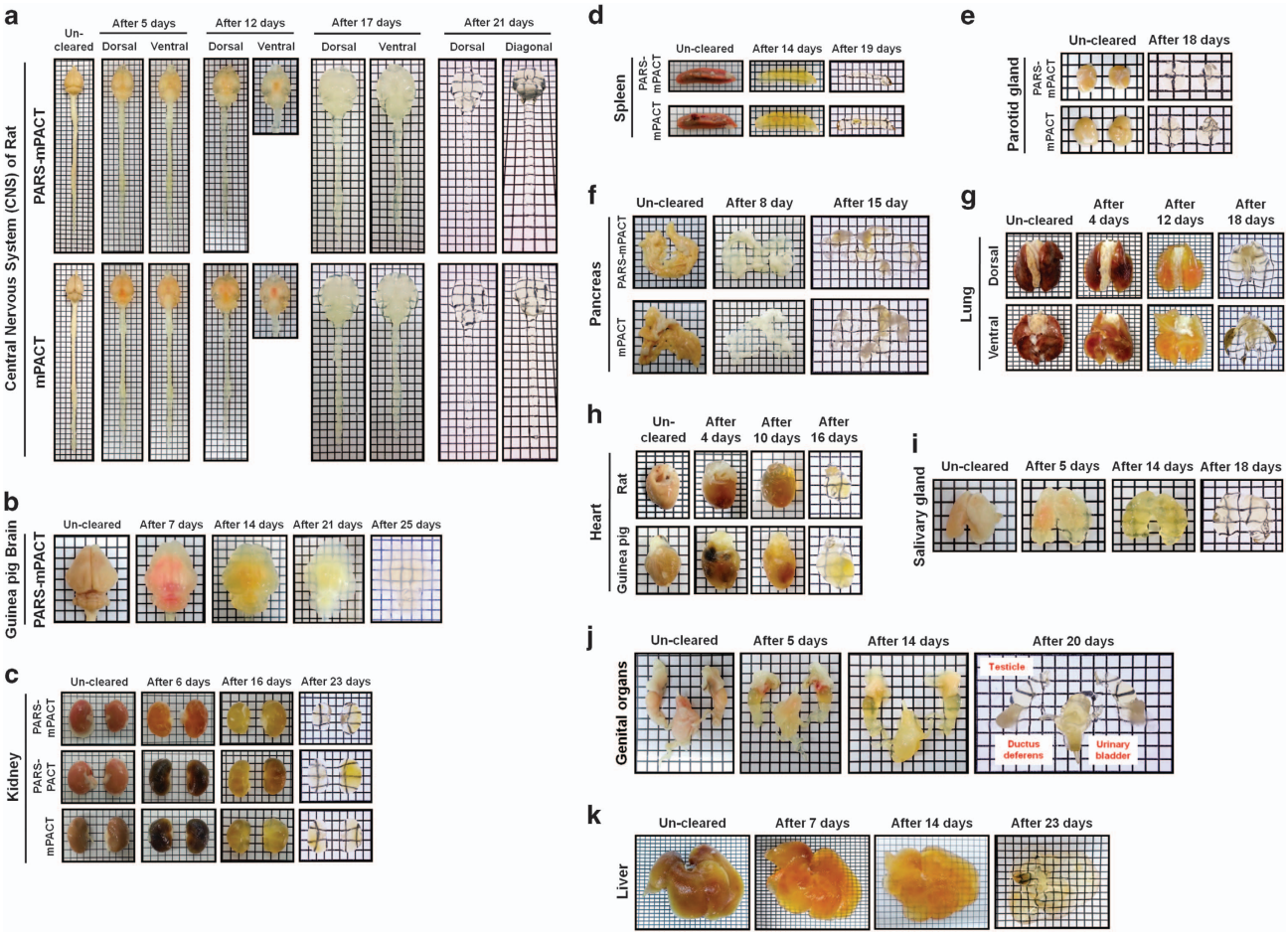

Figure 5 Rat CNS and internal organ clearing performance and comparison of PARS-mPACT and mPACT. (**a**) Optical transparency comparison of the adult rats whole CNS cleared with PARS-mPACT and mPACT. (**b**) Adult guinea pig brain cleared with PARS-mPACT. Left, CNS washed with PBS after fixation with 4% PFA. The transparency of all cleared samples was evident against a patterned background (length:width = 5 mm:5 mm). Optical transparency comparison of the adult rat (**c**) kidney, (**d**) spleen, (**e**) parotid gland and (**f**) pancreas using PARS-mPACT and mPACT clearing. (**g**) Lung (ventral and dorsal), (**h**) adult rat and guinea pig hearts, (**i**) genital organs (testicle, ductus deferens, and urinary bladder), (**j**) salivary gland and (**k**) whole liver cleared by PARS-mPACT. Left, organ washed with PBS after fixation with 4% PFA. The transparency of all cleared samples was evident against a patterned background (length: width = 5 mm:5 mm).

The results demonstrated that mPACT allows high-resolution imaging of cleared whole CNS tissue and other mouse organs. This method also reduced the clearing time to approximately 5–10 days for each organ compared with the longer clearing time required by the original PACT method. We compared the clearance of 4-mm thick rat brain slices using three methods and found that the mPACT method achieved maximal tissue clearing in the shortest time. For the first time, we generated an optically transparent model of a whole rodent CNS with an intact brain and spinal cord using passive clearing.

This study also demonstrated the applicability of the psPACT and mPACT methods for clearing various internal organs, including the whole liver, lung, heart, stoma, salivary glands and pancreas. We optimized the parameters for achieving efficient and consistent tissue clearing and developed stable and rapid tissue-clearing conditions without using electrolysis.

Our study also generated a transparent model of mouse embryos of different developmental stages (E.9.5–E.13.5) using the mPACT method and visualized blood vessel patterns within the notochord. The mPACT protocol rapidly cleared whole organs and required minimal clearing time. In addition, such models could be used to examine the epigenetic aspects of expression and the methylation status of cancer in transgenic embryos.[12–15]

The whole perfusion technique was an important step in the majority of previously reported tissue-clearing techniques.[11] Cardiac perfusion allows the deep infusion of reagents into target tissues in rodents. Based on this feature, the PARS technique enabled the whole-body clearing of mice by whole-organ perfusion.[9] We incorporated the stable features of PARS for more efficient clearing of rat organs and modified it to develop an improved mPACT technique hereby referred to as PARS-mPACT. Using the PARS-mPACT method, we generated transparent models of the whole CNS and a variety of

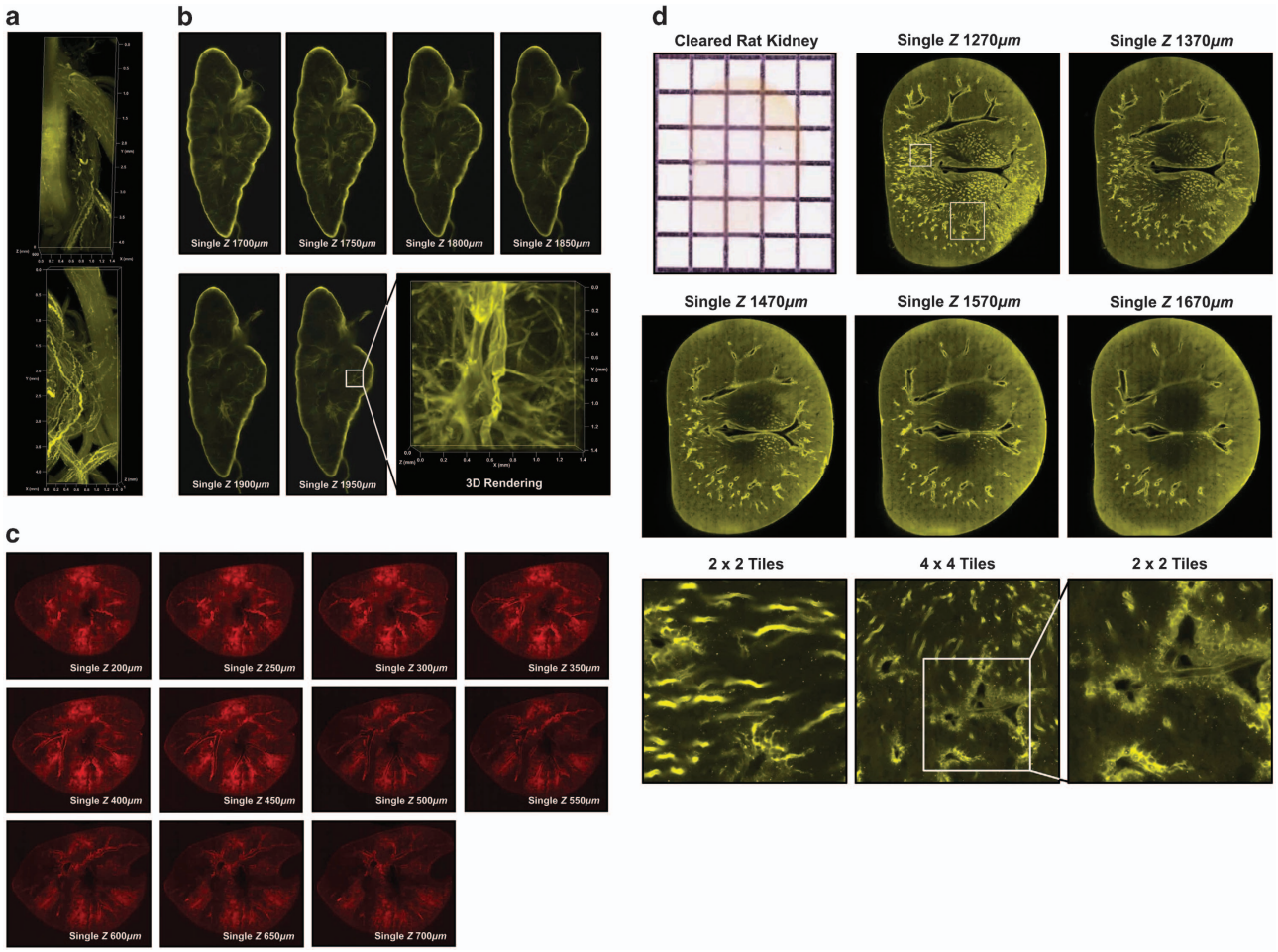

Figure 6 Blood vessel imaging of the lumbar spinal nerves in the cleared spleen and lung of adult rats. Four-millimeter cross-sections of a PARS-mPACT-cleared adult rat spleen and whole caudal lung lobe were stained with anti-CD31 primary antibody to label blood vessels. (**a**) 3D projection of the blood vessel pattern focusing on the lumbar spinal nerve region, including the cauda equine; the top ($z=500$ μm) and bottom ($z=900$ μm) images were 1×3 tiled. (**b**) Spleen, acquired serial single *z*-images ($z=1700$–1950 μm, yellow color) of 36 (4×9, horizontal × vertical tiles) tiled scan images and a 3D projection image of the *z*-stack ($z=350$ μm imaging stack depth). (**c**) Whole caudal lobe of the lung, serial single *z*-images ($z=200$–700 μm, red color) of 224 (16×14, horizontal × vertical tiles) tiled scan images using a ×10 objective lens. The cleared rat kidney was created using the PARS-mPACT method and sectioned to 4-mm thickness. (**d**) The transparency of the cleared rat kidney was evident against a patterned background (length:width = 5 mm:5 mm). The samples are shown after immunostaining with anti-CD31 and Cy3 antibodies and incubation in *n*RIMS, and they showed transparency (top left). The whole image of each sample was created from serial single *z*-images of the blood vessel pattern using confocal microscopy, and the microscope was focused on 2×2 and 4×4 panels, which were tiled (bottom panel).

internal organs, including the whole kidney, spleen, pancreas, parotid gland, lung, heart, salivary gland, genital organs and whole liver of adult rats and guinea pigs. We determined the optimal experimental conditions and compared the clarity of samples processed via PARS-mPACT and mPACT alone. With the PARS method, the whole rat CNS and various other internal organs were cleared without significant compromises in tissue integrity. We speculated that it might be possible to achieve further bone transparency using passive clearing techniques. A fast bone-clearing technique called PACT-deCAL was recently described.[10] Our study attempted to completely remove calcium salt from bone prior to tissue clearing by applying a deCAL process to PARS-mPACT, and we successfully cleared the bone. We named this method PARS-deCAL-mPACT and used it to image 3D blood vessel patterns. Our outcomes were similar to those obtained with the PACT-deCAL method.[10] Although the PARS-deCAL-mPACT method was optimized for microstructure stability of bone tissue following bone clearing by whole perfusion using techniques such as the PARS method, the decalcified bone later showed some damage, implying that further optimization is required to achieve optimal bone clearing while preserving a stable bone structure.

The mPACT method included a lipid wash out of the CNS and various organs, which led to differences in transparency and tissue stability between the general PACT and mPACT methods. In addition, our results suggest a powerful investigative tool for blood vessel networks in organs using 3D analysis

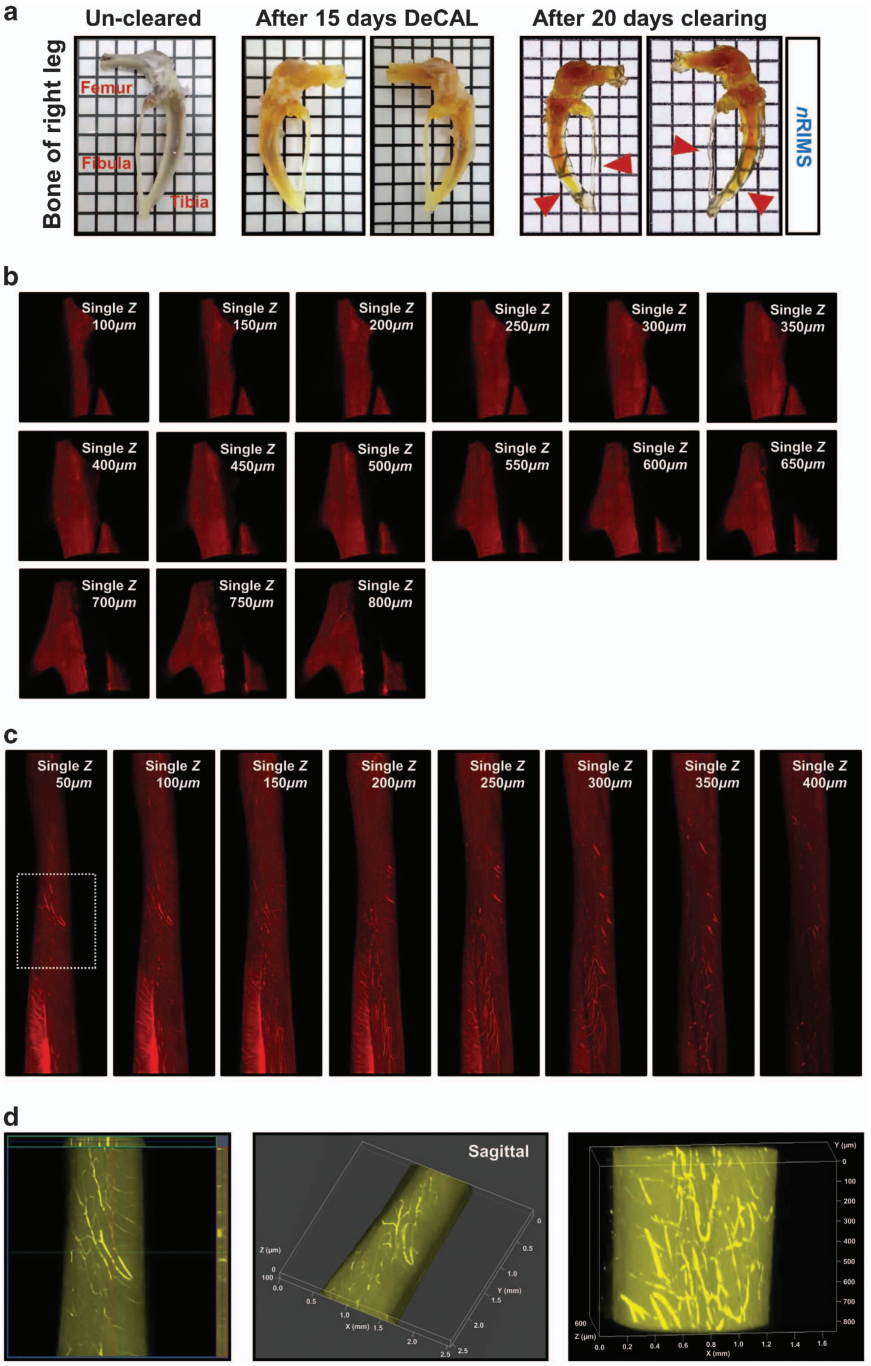

Figure 7 Clearing and visualization of the bone. (**a**) Optical transparency of an adult rat right leg bone following PARS-deCAL-mPACT. Left, the uncleared bone before the PARS method. Middle panel, decalcification 15 days later. Right, the bone cleared with 8% SDS solution for 20 days was imaged with a black cross lattice (width 5 mm) as the background. The red arrows clearly indicate the regions of the fibula and tibia. The PARS-deCAL-mPACT-cleared adult rat leg bone was stained with anti-CD31 primary antibody to label blood vessels. (**b**) The connecting region of the fibula and tibia is indicated by a red arrow in (**a**) in acquired serial single *z*-images ($z = 100$–800 μm, red color) of 64 (8×8, horizontal × vertical tiles) confocal tile scan images. (**c**, **d**) Fibula, serial single *z*-images ($z = 50$–400 μm, red color) of 30 (3×10, horizontal × vertical tiles) tiled scan images and 3D projection image *z*-stack ($z = 110$ μm and 600 μm imaging stack depth, yellow color) obtained using a ×10 objective lens. The transparency of the cleared bone was evident against a patterned background (length:width = 5 mm:5 mm).

of organs in experimental animals. Furthermore, mPACT facilitates the rapid examination of 3D morphological and therapeutic aspects of surgical animal disease models and can be used to aid in the investigation of medical conditions, such as serious injury, malformation, tumors and cancers of various organs.

In conclusion, our mPACT method significantly improves the optical transparency of tissues, is faster than traditional

passive clearing methods and requires limited equipment and minimal hands-on processing time. Our data suggest that mPACT and PARS-mPACT could help to provide access to stereoscopic multiscale information that will expand current understanding of health and disease.

CONFLICT OF INTEREST

The authors declare no conflict of interest.

ACKNOWLEDGEMENTS

We thank Professor Sung-Wook Kuh, Professor Jeong-Yoon Park, Dr Zahid Hussain at the Yonsei University College of Medicine and Eunice Yoojin Lee at the Columbia University College of Physicians and Surgeons for their helpful comments on this manuscript. This work was supported by the Brain Korea 21 PLUS Project for Medical Science, Yonsei University. In addition, this work was supported by a grant from the Interalia Foundation (6-2013-0161).

Author contributions: JW conceived the mPACT and PARS-mPACT methods and designed all experiments. JW and ML designed and performed multiplexed staining and imaging experiments. HP contributed to the CLARITY experiments. JW and JS wrote the manuscript. YC supervised all aspects of the work.

1 Chung K, Wallace J, Kim SY, Kalyanasundaram S, Andalman AS, Davidson TJ *et al.* Structural and molecular interrogation of intact biological systems. *Nature* 2013; **497**: 332–337.
2 Tomer R, Ye L, Hsueh B, Deisseroth K. Advanced CLARITY for rapid and high-resolution imaging of intact tissues. *Nat Protoc* 2014; **9**: 1682–1697.
3 Hama H, Kurokawa H, Kawano H, Ando R, Shimogori T, Noda H *et al.* Scale: a chemical approach for fluorescence imaging and reconstruction of transparent mouse brain. *Nat Neurosci* 2011; **14**: 1481–1488.
4 Ke MT, Fujimoto S, Imai T. SeeDB: a simple and morphology-preserving optical clearing agent for neuronal circuit reconstruction. *Nat Neurosci* 2013; **16**: 1154–1161.
5 Kuwajima T, Sitko AA, Bhansali P, Jurgens C, Guido W, Mason C. ClearT: a detergent- and solvent-free clearing method for neuronal and non-neuronal tissue. *Development* 2013; **140**: 1364–1368.
6 Susaki EA, Tainaka K, Perrin D, Kishino F, Tawara T, Watanabe TM *et al.* Whole-brain imaging with single-cell resolution using chemical cocktails and computational analysis. *Cell* 2014; **157**: 726–739.
7 Murray E, Cho JH, Goodwin D, Ku T, Swaney J, Kim SY *et al.* Simple, scalable proteomic imaging for high-dimensional profiling of intact systems. *Cell* 2015; **163**: 1500–1514.
8 Lee H, Park JH, Seo I, Park SH, Kim S. Improved application of the electrophoretic tissue clearing technology, CLARITY, to intact solid organs including brain, pancreas, liver, kidney, lung, and intestine. *BMC Dev Biol* 2014; **14**: 48.
9 Yang B, Treweek JB, Kulkarni RP, Deverman BE, Chen CK, Lubeck E *et al.* Single-cell phenotyping within transparent intact tissue through whole-body clearing. *Cell* 2014; **158**: 945–958.
10 Treweek JB, Chan KY, Flytzanis NC, Yang B, Deverman BE, Greenbaum A *et al.* Whole-body tissue stabilization and selective extractions via tissue-hydrogel hybrids for high-resolution intact circuit mapping and phenotyping. *Nat Protoc* 2015; **10**: 1860–1896.
11 Tainaka K, Kubota SI, Suyama TQ, Susaki EA, Perrin D, Ukai-Tadenuma M *et al.* Whole-body imaging with single-cell resolution by tissue decolorization. *Cell* 2014; **159**: 911–924.
12 Lubet RA, Zhang Z, Wiseman RW, You M. Use of p53 transgenic mice in the development of cancer models for multiple purposes. *Exp Lung Res* 2000; **26**: 581–593.
13 Macleod KF, Jacks T. Insights into cancer from transgenic mouse models. *The J Pathol* 1999; **187**: 43–60.
14 Ritorto MS, Rhode H, Vogel A, Borlak J. Regulation of glycosylphosphatidylinositol-anchored proteins and GPI-phospholipase D in a c-Myc transgenic mouse model of hepatocellular carcinoma and human HCC. *Biol Chem* (e-pub ahead of print 28 June 2016; doi: 10.1515/hsz-2016-0133).
15 Hohenauer T, Moore AW. The Prdm family: expanding roles in stem cells and development. *Development* 2012; **139**: 2267–2282.

Supplementary Information accompanies the paper on Experimental & Molecular Medicine website (http://www.nature.com/emm)